Boron and lithium behaviour in river waters under semiarid climatic conditions

V Censi, Pierpaolo Zuddas, F Sposito, M Cangemi, C Inguaggiato, D Piazzese

Contents lists available at ScienceDirect

Chemosphere

journal homepage: www.elsevier.com

Boron and lithium behaviour in river waters under semiarid climatic conditions

V. Censi [a], P. Zuddas [b], F. Sposito [c], M. Cangemi [a], C. Inguaggiato [d], D. Piazzese [a, *]

[a] DiSTeM, University of Palermo, Via Archirafi 22, 90123, Palermo, Italy
[b] Sorbonne Université, CNRS, METIS, F75005, Paris, France
[c] INGV (Palermo Section), Via U. La Malfa 153, 90146, Palermo, Italy
[d] Departamento de Geología, Centro de Investigación Científica y de Educación Superior de Ensenada (CICESE), Carretera Ensenada-Tijuana, 3918, Ensenada, Baja California, Mexico

ARTICLE INFO

Handling Editor: Milena Horvat

Keywords:
Mine drainage
Salt minerals
B/Li ratio
Ionic strength
Mn-oxyhydroxides

ABSTRACT

Boron (B) and Lithium (Li) concentrations were studied in the Platani river, one of the most important catchments of South-Central Sicily which is under semiarid climatic conditions for roughly eight months to a year. In this area, evaporites result in potential B and Li sources for surface waters. Results from river waters have measured ionic strength values between 0.1 and 4.54 M. B and Li distributions in these waters were studied in colloidal (CF, extracted by ultrafiltration from the 0.45 μm filtrate) and total dissolved (TDF) fractions and in fractions extracted from corresponding riverbed sediments, according to changes of the B/Li ratio.

In river waters, CF and TDF showed very similar B/Li values, suggesting that only negligible fractionation occurs between Li and B in the aqueous phase. Similar evidence was observed between B/Li values in TDF and the labile sediment fraction, whereas an inverse relationship arose between B/Li values in TDF and in the easily reducible sediment fraction. This relationship indicates that Mn oxy-hydroxides preferentially react with aqueous B species relative to Li at the riverbed sediment interface.

The extent of the B–Mn oxy-hydroxide reactions is influenced by the ionic strength, so that only B/Li values below 4 are measured in river waters with ionic strength values above 0.5 M. Comparing B/Li and ionic strength values measured in the Platani river with those from oxic brines worldwide, the same preferential B removal relative to Li is observed. This evidence suggests that B is removed as positively-charged borate ion-pairs, formed in the aqueous phase under higher ionic strength conditions, reacting with negatively charged surfaces of Mn oxy-hydroxides. The observed B reactivity relative to Li could be exploited to bring down the B excess from natural or waste waters, allowing the natural reactions with Mn oxy-hydroxides to take place under natural conditions.

Author contribution statement

Conceptualization: P. Zuddas, D. Piazzese, C. Inguaggiato, V. Censi. Data curation: M. Cangemi, D. Piazzese,V. Censi. Formal analysis: P. Zuddas, D. Piazzese, V. Censi. Funding acquisition: D. Piazzese. Investigation: F. Sposito, V. Censi, C. Inguaggiato. Methodology: M. Cangemi, D. Piazzese, V. Censi. Software: V. Censi. Supervision: P. Zuddas, D. Piazzese, Validation: D. Piazzese, V. Censi. Visualization: M. Cangemi, D. Piazzese, V. Censi. Writing – original draft: P. Zuddas, D. Piazzese, V. Censi. Writing – review & editing: P. Zuddas, M. Cangemi, D. Piazzese, V. Censi.

1. Introduction

B and Li are light elements that are geochemically incompatible with minerals during magmatic crystallisation, and they are enriched in fluids during rock-water interactions (Cullen et al., 2019; Godfrey et al., 2019; Ryan and Langmuir, 1993). In natural waters, B occurs as $[H_3BO_3]^0$, whereas $[B(OH)_4]^-$ ion prevails under alkaline conditions and shows limited reactivity towards surfaces of clays, carbonates, and metal oxides (Goldberg, 1997; Vengosh et al., 1998). Li usually occurs as an aqueous metal ion that shows a limited affinity toward clay mineral surfaces (Millot et al., 2010; Hoyer et al., 2015; Stoffyn and Mackenzie, 1982; Sun et al., 2021).

* Corresponding author.
Email address: daniela.piazzese@unipa.it (D. Piazzese)

https://doi.org/10.1016/j.chemosphere.2022.135509
Received 27 April 2022; Received in revised form 7 June 2022; Accepted 25 June 2022
Available online xxx
0045-6535/

The stability of these aqueous species and the corresponding limited affinity towards solid surfaces result in average B and Li concentrations in rivers and surface waters worldwide spanning a range within 0.1–10 and 0.001–1.5 μM, respectively (Gaillardet et al., 2013; Hasenmueller and Criss, 2013). During evaporation, dissolved Li and B are usually conservatively enriched. Correspondingly, B and Li concentrations can attain very high values, up to 39.6 and 52 mM, respectively, in brines from evaporitic basins and entrapped in voids and fluid inclusions during the formation of salt deposits (McCaffrey et al., 1987; Godfrey et al., 2019; Godfrey and Álvarez-Amado, 2020; Zilberman et al., 2017). Accordingly, natural brines are considered to be the most promising industrial sources for B and Li extraction (Godfrey and Álvarez-Amado, 2020; Parans Paranthaman et al., 2017).

B is an essential micronutrient for vital processes, but it becomes toxic for plants, animals, and humans exposed to high concentrations (Ince et al., 2017; Wang et al., 2021). Li is considered to play a pivotal role in some biochemical processes, especially during foetal development (Schrauzer, 2002), but excess Li from some vegetables can result in neurotoxicity, depending on location and type of food (Domínguez Ortega et al., 2006).

Accordingly, B and Li pollution represents an environmental risk for surface and groundwater. This is highlighted by the aqueous stability of B and Li species and their limited reactivity during rock-water interactions. Potential sources of B and Li pollution are wastewaters from the industrial treatment of B and Li (Deng et al., 2021), drain waters from salt mine landfills (Godfrey and Álvarez-Amado, 2020), deep groundwaters from sedimentary basins (Sanjuan et al., 2022) and shale gas hydraulic fracturing back-flow (Cozzarelli et al., 2017). Similar scenarios can be very dangerous, especially in arid and semiarid environments where freshwater quality and availability are important (Babiker et al., 2019). In southern European surface waters, B concentrations up to 140 μM (Kochkodan et al., 2015) higher than the fixed threshold for drinking and agricultural waters (corresponding to 50 μM) were measured (WHO, 2017). This evidence can be considered to be a consequence of progressive climatic changes toward subarid conditions in some areas of southern Europe (Navarro-Martínez et al., 2020).

Accordingly, the aim of this study is to recognise the B and Li distribution between colloids and the total dissolved fraction in a river system under semiarid conditions and to determine what processes can influence the mobility of these elements at the riverbed sediment-water interface. In South-Central Sicily, the Platani river is a suitable context to carry out this study. River waters represent one of the most important sources of surface water for agricultural purposes. Moreover, large evaporitic out-crop deposits and a large salt landfill that occur in the Platani catchment represent suitable B and Li sources to study the behaviour of these elements in a river under semiarid conditions.

2. Geological and hydroclimatic outlines

The Platani River catchment (1785 km^2) is located in South-central Sicily within the Caltanissetta Basin (see Fig. 1), and it is NE-SW oriented in the same area where Messinian evaporites form the main outcrops. These evaporites consist of carbonate units and gypsum with different textures. In places, native sulphur deposits are embedded be-

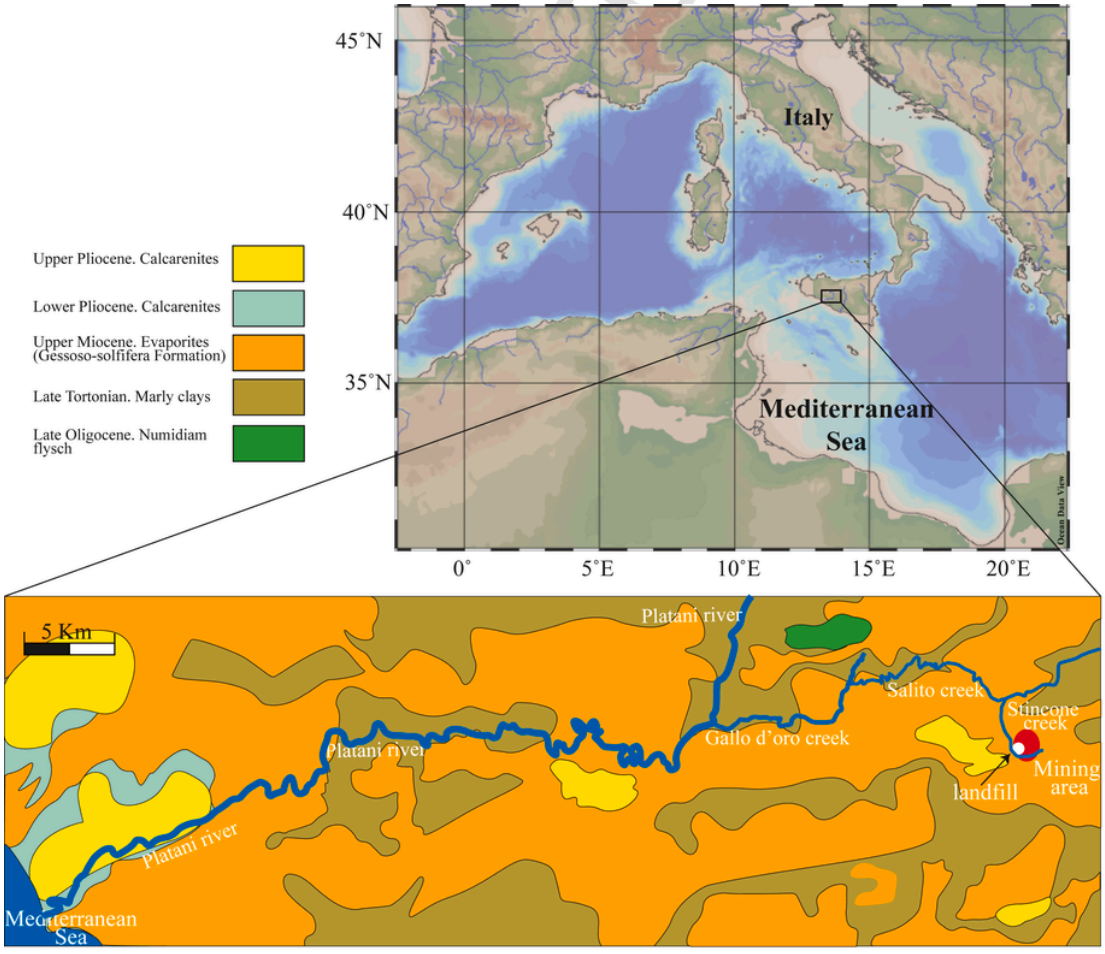

Fig. 1. Geographical sketch-map illustrating Central Sicily (redrawn from Ocean Data View™ software, Schlitzer, 2015) and the studied area corresponding to the Platani river watershed. Here, the given geological map illustrates main outcrops occurring in the Platani river watershed and the site of Bosco-S. Cataldo mine.

tween the carbonate and gypsum strata (Dessau et al., 1962). In some areas, the evaporite sequence is topped by large Na–K salt deposits. The mining industry has been exploiting sulphur deposits in this area starting from the Roman Age, and this has continued up to the '60s. Subsequently, the mining activity was converted to salt exploitation, mainly kainite ($KClMgSO_4 3H_2O$) and halite, and it currently continues in some selected areas. In the Bosco San Cataldo area, the remnant of abandoned mining activities left a landfill formed primarily of about 5 million cubic meters of halite and secondly of potash salts. Waters of the Stincone creek, flowing at the base of the landfill, progressively leach salts. This results in high B and Li concentrations in the upper part of the Platani river stem.

The climate in South-Central Sicily is hot and dry for 6–8 months out of the year. About 135 mm of rainwater fall between April and September. Corresponding average temperatures span from 15.8 to 26.8 °C. On the contrary, about 480 mm of rainwater fall between October to March when average temperatures between 12.2 and 20.9 °C are measured. During the winter, the weather is moderately cold and rainfall increases, becoming abundant mainly at altitudes above 1000 m. Under these conditions, the drainage system is full of water.

3. Methods

3.1. Sampling

The Platani River is the second widest drainage basin in South-Central Sicily. It has three main tributaries (Gallo d'Oro, Salito and Stincone) and a total flow rate close to 31.5 $*10^6 m^3 y^{-1}$ (Fig. 1). Thirty water samples and twenty-five sediment samples were collected along the Platani River from the Bosco San Cataldo mine. Water and sediment samples were taken mainly along the small tributaries of the Platani River with shallow water depths and a turbulent flow regime with suspended particles (> 450 nm) derived from resuspension of the riverbed sediments. Sampling was carried out from December 2014 to October 2016. The temperature, Eh, pH, and electrical conductivity were measured in the field using portable ORION instruments, while alkalinity was titrated in the field with 0.1 M HCl. Eh values were corrected for the temperature. The pH meter was calibrated with three buffers having nominal pH 4.01, 7.00 and 9.95 at 25 °C. After the addition of a NaCl 5 M solution in each buffer, their pH measurements were carried out another time and these new values used to calibrate the pH meter (Nir et al., 2014).

Samples for major ion determinations were collected using 50 ml LD-PE double-capped bottles. The samples were filtered with 0.45 μm Millipore MF filters and acidified with HNO_3. Three litres of water for each site were collected and immediately filtered through a 0.45 μm sterile filter membrane (CHM™ cellulose acetate filter) and stored in Nalgene™ bottles. One litre was acidified to pH ≈ 2 with 1% ultra-pure HNO_3 for dissolved fraction (DF) measurements, while the other 2 L didn't undergo any further field treatments.

3.2. Aqueous analysis and calculations

Major ion concentrations were measured using a Dionex ICS 1100 chromatograph equipped with a CS-12A column for cations and an AS14A column for anions. The untreated 2 L were used for separating colloids (CF) from the total dissolved fraction (TDF) by tangential ultrafiltration using a VIVAFLOW 50R® (Sartorius Stedim Biotech GmbH) cross-flow filtration cassette manifold (molecular weight cut-off 10 KDa) with a 50 cm^2 filter surface area and regenerated cellulose filters.

The concentration factor (C_f) > 10 was calculated for the colloidal fractions using the following equation:

$$cf = \frac{(Volume_{TDF}) + (Volume_{CF})}{(Volume_{CF})} \quad (1)$$

(Larsson et al., 2002; Guo and Santschi, 2007). After separation, the aliquot for TDF was acidified with 1% ultra-pure HNO_3 solution to attain pH ≈ 2, and then it was stored for analysis. B and Li concentrations were determined by Quadrupole-ICP-MS (Agilent 7800 cc) with a classical external calibration procedure.

The water saturation state was calculated by PHREEQC software (version 3.0.6; Parkhurst and Appelo, 2010) using the LLNL correcting stability constants of investigated complexes (Byrne and Kester, 1974; Vengosh et al., 1991) for the salinity. According to Tepavitcharova et al. (2011), the thermodynamic pitzer. dat database was used for assessment of the saturation state and B speciation in water samples having ionic strength above 0.1 M (Nir and Lahav, 2015).

The saturation state for several minerals was assessed. In particular, calcite, dolomite, aragonite, anhydrite, gypsum, barite, goethite, boehmite, kaolinite, montmorillonite and halite were considered. According to Lewis and Randall (1921), the ionic strength was assessed as:

$$\mu = \frac{1}{2}\sum_i m_i Z_i^2 \quad (2)$$

where m_i is the molality of the *i*th ion and Z_i its ionic charge.

3.3. Riverbed sediments

Riverbed sediments were analysed by X-ray diffraction (XRD) at different size fractions (see Supplementary Figure S1), while a sequential extraction methodology was used to identify possible different reactive phases. The selected methodology consisted of different stages that allowed us to identify four different reactive fractions of the sediment (Koschinsky and Halbach, 1995). This was preferred to the classical approach from Tessier et al. (1979) because it provides an extraction protocol that differentiates trace elements bounded to Mn-oxides from those bounded to Fe oxides.

1. *Labile fraction extraction*: 1 g of powdered sample was added to a solution of 30 ml of 1 M acetic acid, buffered with Na acetate, at room temperature for 5 h. After the reaction, the resulting solution was filtered with a 450 nm membrane and brought up to a final volume of 50 ml.
2. *Easily reducible fraction extraction*: 175 ml of a solution of 0.1 M hydroxylamine hydrochloride (pH 2) was added to the residual sediment from the previous step and stirred for 24 h at 25 °C. The resulting solution was separated from the residual sediment as in step 1 and brought up to a final volume of 200 ml.
3. *Moderately reducible fraction extraction*: the solid residue of step 2 was treated with 175 ml of 0.2 M oxalic acid, buffered with ammonium oxalate (pH 3.5), and stirred at 25 °C for 12 h. The resulting solution was separated from the residual sediment as in step 1 and brought up to 200 ml final volume (Koschinsky and Halbach, 1995).
4. *Residual-silicate fraction extraction*: The solid residue from the previous steps was fully digested in Teflon bombs at 180 °C for 12 h with a solution of 3 ml of 48% HF, 3 ml of 37% HCl, and 1 ml of 65% HNO_3. After digestion, the solution was filtered, and Millipore water was diluted to 50 ml.

In our protocol procedure, the leaching solution from the first step contains labile-bounded trace elements related to soluble carbonate minerals. Elements of step 2 are attributed to Mn-bearing phases (Mn-oxyhydroxides), while elements measured in step 3 are assumed to represent trace elements released from Fe-bearing phases. Finally, step 4 represents elements associated with the detrital component of sediments. The solution composition obtained from the selected sequential extraction procedure was analysed as a water sample.

The assessment of fractions extracted from sediments was carried out as follows. The sum of B and Li concentrations in measured in each fraction extracted from the sediment represents the overall B and Li concentration occurring in each sediment sample ($([B] + [Li])_{Wsed}$:

$$([B] + [Li])_{sed1} + ([B] + [Li])_{sed2} + ([B] + [Li])_{sed3} + ([B] + [Li])_{sed4} = ([B] + [Li])_{Wsed} \quad (3)$$

where the subscripts from sed 1 to sed 4 in eqn. (3) indicate the 1st, 2nd, 3rd and 4th fractions extracted from each sediment. According to eqn. (1), the percent of each sediment fraction can be assessed and reported in the Supplementary Table 3.

4. Results

4.1. Aqueous geochemistry

The major composition of dissolved elements measured in TDF from river waters is reported in Supplementary Table 1 and depicted in Fig. 2. This figure shows that two distinct water groups can be identified by the major composition of the dissolved elements of the river waters (Supp. Table 1, Fig. 2). Starting from the alkaline metal/chloride corners representing the composition of materials forming the mine landfill (Fig. 2A and B), trends 1 are addressed to the Mg^{2+} and SO_4^{2-} graph corners, whereas trends 2 are directed towards the Ca^{2+}, $HCO_3^- + CO_3^{2-}$ graph corners. Group-1 waters are those collected along the Stincone creek from the landfill down to the junction with the Salito creek. Group-2 waters are those collected downstream of the Stincone-Salito creek junction. These pieces of evidence suggest that the major element concentration of Group-1 waters is influenced by salt weathering from the landfill mainly along the Stincone creek, whereas the composition of Group-2 waters is also influenced by the leaching of evaporitic carbonates and gypsum. Group 1 waters have ionic strengths μ from 0.2 to 4.54 M, pH close to 8, overall Ca^{2+} and Mg^{2+} concentrations higher than 35 mM, and Eh values between −0.025 and 0.2 V. Group 2 waters have lower μ values, from 0.09 to 0.69 M, and pH and Eh values similar to Group 1.

Saturation calculation reveals that Group 1 waters are mainly saturated or oversaturated concerning carbonates (calcite and dolomite) and clay-minerals (kaolinite and smectites), whereas Group 2 waters are additionally saturated in barite and goethite. We also found that $[B(OH)_3]^0$ is the more abundant B species in the studied waters, while $Me(B(OH)_4)]^+$ borate ion-complexes are significant when Ca^{2+} or Mg^{2+} concentrations are higher. Accordingly, the $[B(OH)_3]^0/[Me(B(OH)_4]^+$ ratio is 2 times higher in Group 2 when compared to Group 1 waters.

In the dissolved fraction (Supplementary Table 2), B and Li concentrations span between 190.6 and 402.2 μM and between 41.2 and 92.7 μM, respectively, yielding distinct B/Li ratios between Group 1 and Group 2. Fig. 3A shows that B versus Li describes a linear trend with a slope of 3.9 ± 0.2 in Group 1, while Group 2 shows a trend with a slope of 11.5 ± 2.5. Plotting the B/Li ratio vs μ (Fig. 3B), we found that the B/Li ratio was spread between 4 and 16 for μ below 1 M, while it remained almost constant at 4 when μ was between 1 and 4 M. This indicates that the ionic strength plays an important role in the fractionation of the dissolved B/Li ratio. Comparing the B/Li ratio in TDF with and the values measured in the corresponding CF (Fig. 3C), a linear trend with a slope close to 1 ± 0.1 is observed. This evidence suggests that B and Li are not fractionated between the dissolved phase and colloids.

4.2. Sediment mineralogy and composition

XRD analysis shows that the coarse sediment fraction (>2 μm) mainly consists of gypsum ($CaSO_4*2H_2O$), calcite ($CaCO_3$), dolomite [$(CaMg(CO_3)_2$], celestine ($SrSO_4$), AlOOH (probably boehmite), and rarely strontianite ($SrCO_3$). The fine fraction (<2 μm) contains montmorillonite [$(Na,Ca)_{0.33}(Al,Mg)_2(Si_4O_{10})(OH)_2*nH_2O$] and kaolinite ($Al_2(OH)_4Si_2O_5$). Diffraction spectra of fine and coarse fractions from representative sediment samples are reported in Supplementary Fig. 1. A similar composition was also found in the suspended solids having diameters >0.45 μm. XRD data did not identify the presence of B and Li minerals in solids from the mine landfill.

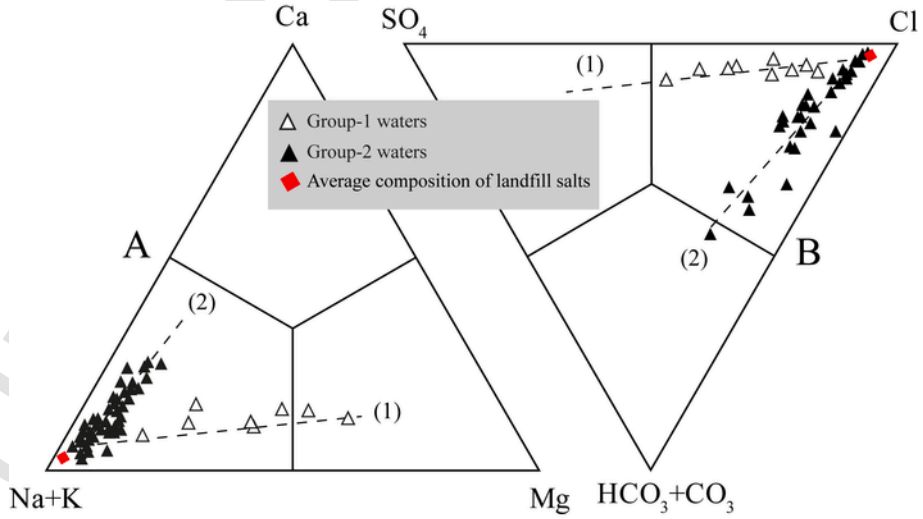

Fig. 2. Ternary plots of major ions of water samples in the Platani river: (A) Major cations; (B) Major anions. The water samples of Group-1 appear in a white triangle, those of Group-2 in a black triangle, a red rhombus indicates an average composition of the landfill salts. Those depicted are suitable trends illustrating the possible evolution of the major element composition in Group-1 and Group-2 waters due to the dissolution of landfill salts and weathering of evaporites outcropping along the river path, respectively. The data on which the illustration is based are reported in Supplementary Table 1. (For interpretation of the references to colour in this figure legend, the reader is referred to the Web version of this article.)

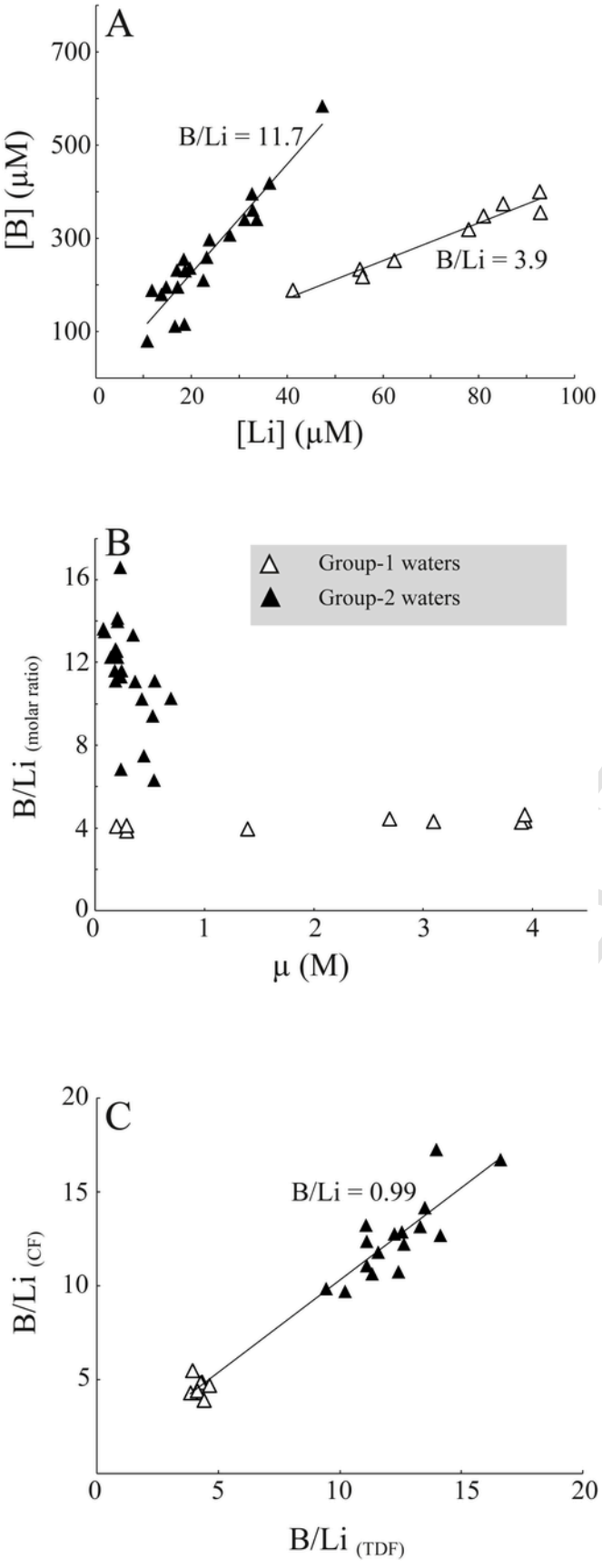

Fig. 3. A: Boron vs. lithium concentrations in Group-1 (white triangle) and Group-2 (black triangle) water samples. B: B/Li ratio measured in the Platani river vs. corresponding ionic strength values. C: B/Li ratio measured in TDF compared with corresponding values measured in CF.

Silicate minerals range between 80% and 95% and constitute the most abundant sediment fraction, whereas the easy soluble (carbonate-rich) fraction represents between 0.5 and 2.5%. The easily reducible (Mn-rich) fraction ranges between 2.1 and 14.6%, and the moderately reducible Fe-rich fraction is between 0.6 and 7.6%.

Fig. 4 shows that in the 1st and 2nd fractions of Group-1 sediments, ranges of Li and B concentrations are narrower than in the corresponding fractions of Group-2 sediments. In both these fractions, Li concentrations are higher in Group-1 than in Group-2 sediments and B/Li values are lower in Group-1 than in Group-2 sediments. In 3rd and 4th fractions of riverbed sediments ranges of Li and B concentrations are similar in Group-1 and Group-2. Only the range of B/Li values is narrower in Group-1 than in Group-2 sediments.

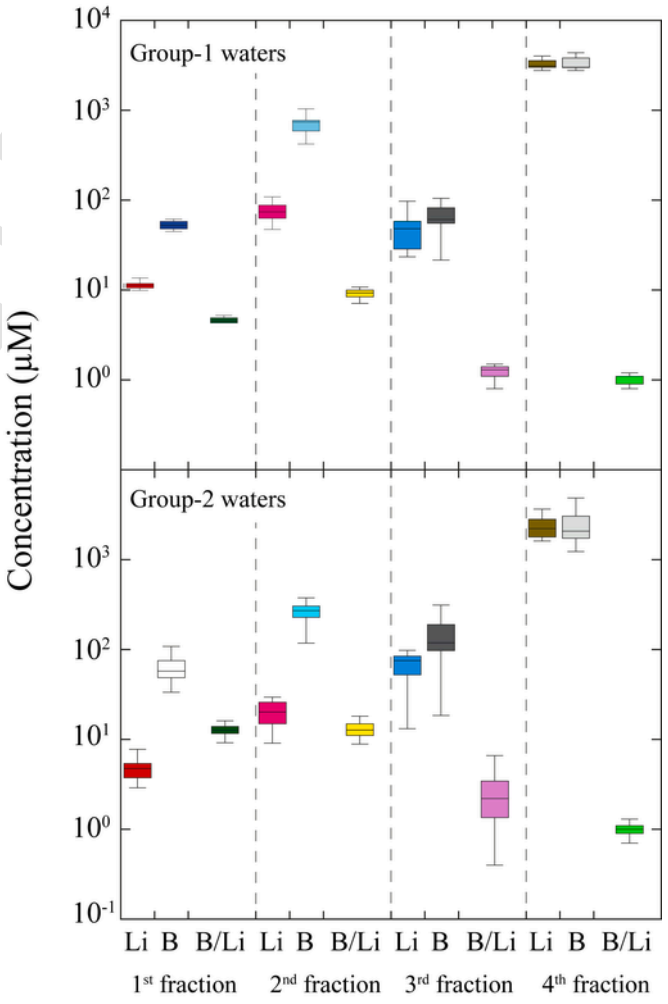

Fig. 4. Box plots illustrating ranges of Li, B concentrations and B/Li values measured in fractions extracted from riverbed sediments corresponding to Group-1 and Group-2 waters.

5. Discussion

5.1. B and Li reactions onto mineral surfaces

Reporting B/Li values measured in the labile sediment fraction vs. corresponding values from TDF, linear trends with slopes of 1.27 and 1.02 are depicted from Group 1 and Group 2 waters, respectively (Fig. 5A). Accordingly, significant differences in aqueous B and Li reactivity towards the labile fraction extracted from riverbed are not shown.

Fig. 5B shows that aqueous B/Li values are inversely related to those measured in the corresponding easily reducible sediment fraction. This evidence suggests that B-species are partitioned onto surfaces of Mn-rich minerals in Group 1 waters. These solids generally have an amorphous or cryptocrystalline nature (Qin et al., 2019) and show high surface reactivity toward dissolved metal species (Stumm, 1992). Since surfaces of Mn-rich minerals are negatively charged under ionic strengths higher than 0.1 M (Tsadilas et al., 1998; Villalobos, 2015; Kosmulski, 2016; Brodskii et al., 2015) and the proportion of positively charged borate ion-complexes is likely more abundant, the observed fractionation of B/Li ratio in Group 1 waters could result from the adsorption of charged B species onto surfaces of Mn-rich minerals. However, this reactive process is likely to be lacking in waters of Group 2 waters that have lower ionic strength. Indeed, aqueous B/Li values are always positively related to those measured in the easily reducible sediment fraction in Group 2 waters.

In the moderately reducible (Fe-rich) sediment fraction, B/Li values are poorly correlated to those measured in the corresponding TDF, both in Group 1 and Group 2 waters (Fig. 5C). There, B/Li values are generally lower in this sediment fraction than in the corresponding TDF. This could reflect the known strong Li affinity for Fe-oxyhydroxide surfaces (Wimpenny et al., 2010a) and the lack of reactivity of B species on the positively charged surface of Fe-oxyhydroxides (Kosmulski, 2002, 2016). Finally, the B/Li ratio in the detrital sediment fraction roughly corresponds to the B/Li crustal value, while both dissolved B and Li species are not partitioned onto surfaces of detrital minerals during authigenic processes (Bhagyaraj et al., 2021), as observed in Fig. 5D.

5.2. B removal in natural water conditions

In the area of Platani river catchment studied, higher B/Li ratios are found in lower ionic strength (Group-2) waters, while lower B/Li ratios are measured in higher ionic strength (Group-1) waters. Concomitantly, the identified preferential scavenging of dissolved B-species (mainly $B(OH)_3$ and $[Me(B(OH)_4]^+$) onto Mn-rich minerals in Group 1 rather than Group 2 waters reflects the inverse relationship between B/Li ratios in TDF and the easily reducible sediment fraction of Group-1 waters (Fig. 5B). Assuming the Mn oxy-hydroxide surfaces are negatively charged at pH values above 3.5 (Brodskii et al., 2015; Kosmulski, 2016), the observed preferential removal of B would result from the reaction of positively charged aqueous B species ($[B_{aq}]^+$) with the reactive sites of the negatively charged surface of Mn-oxides ($[MnOX]^- >$) according to the following schematic process:

$$[MnOX]^- > + [B_{aq}]^+ \leftrightarrow [MnOX > B_{aq}] \quad (4)$$

Positively charged aqueous B species ($[B_{aq}]^+$) would correspond to $[Me(B(OH)_4)]^+$ borate-ion complexes that would be formed through the following reaction under high ionic strength conditions:

$$Me^{2+} + B(OH)_3 + H_2O \leftrightarrow MeB(OH)_4^+ + H^+ \quad (5)$$

Fig. 6 compares the distribution of B/Li values vs. the ionic strength in Platani waters with values measured in some high salinity oxic wa-

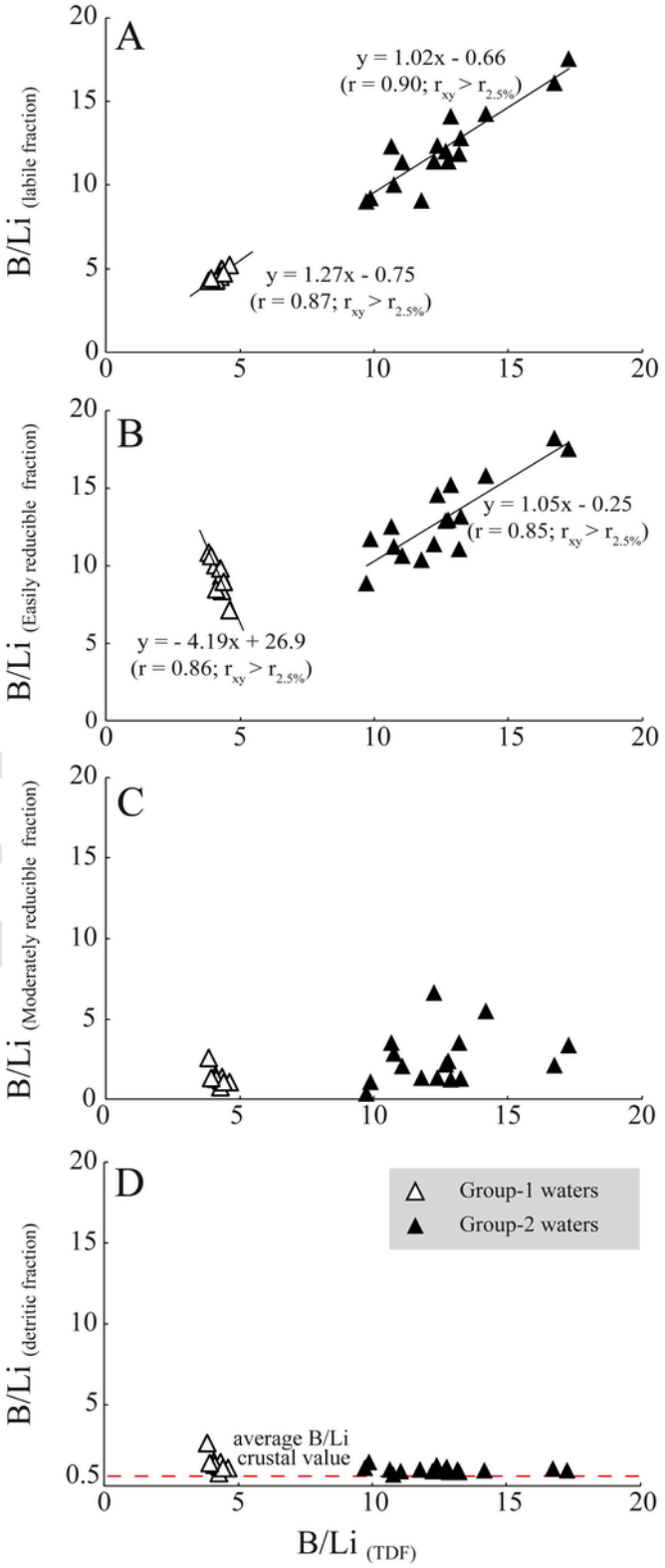

Fig. 5. B/Li ratio measured in the dissolved fraction of studied waters compared with corresponding values in labile (carbonate-rich) fraction (A), in the easily reducible (Mn-rich) fraction (B), in the moderately reducible (Fe-rich) fraction (C) and detritic fraction (D) of the corresponding river sediments. In Fig. 4D the average B/Li crustal value is reported for reference.

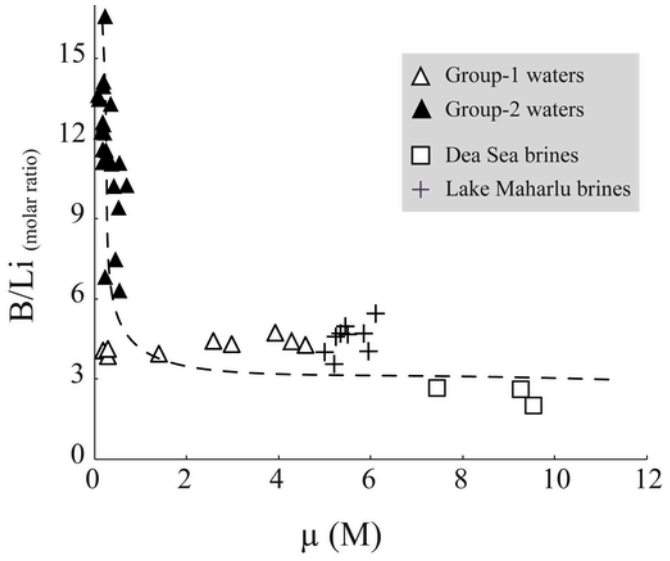

Fig. 6. B/Li ratio measured in studied river waters vs. their ionic strength compared with corresponding values from Lake Maharlu (Khosravi et al., 2019) and the Dead Sea brines (Vengosh et al., 1991). The dashed line corresponds to Eq. (4).

ters in equilibrium with Mn oxy-hydroxides from the Dead Sea and the Maharlu lake (Gavrieli and Halicz, 2002; Herut et al., 1997; Khosravi et al., 2019; Nishri and Nissenbaum, 1993). The observed distribution depicts the following empirical relation:

$$\frac{B}{Li} = \frac{3.2\,(\pm 0.6)\,\mu}{\mu - 0.122\,(\pm 0.006)} \quad (6)$$

The right-hand term of Eqn. (6) formerly looks like the Monod-like equation (Roden, 2008) where the ionic strength μ would play the same limiting role of the substrate concentration during microbial-controlled reactions (Brantley and Conrad, 2008). Accordingly, this evidence suggests that the ionic strength can play a limiting role towards changes in the B/Li ratio, consistent with the influence that the ionic strength exercises through Ca^{2+} and Mg^{2+} concentrations in the formation of borate-ion complexes (see Eqn. (5)). Therefore, we propose that the observed removal of B from the aqueous phase described in Eqn. (2) may result from the formation of borate ion-complexes under high ionic strength that would represent the rate-limiting step of the overall process. Mineral dissolution through mine landfill weathering favours high Ca^{2+} and Mg^{2+} contents, mainly in Group 1 waters, in turn enhancing the formation of borate ion pairs therein.

The reactivity of aqueous B species on surfaces of Mn-rich solids corresponds to experimental evidence of B reactivity on $Mg(OH)_2$, Mn-, or Fe oxyhydroxide surfaces (Babiker et al., 2019; Bingham and Page, 1971; Mandal and De, 1993). Recently, the preferential ability of Mn-oxyhydroxide surfaces to capture positively charged B ions was also confirmed by Elmaci et al. (2015). They were studying the ^{11}B versus ^{10}B fractionation at high ionic strength when borate charged ion-complexes are abundant. Moreover, Mn oxyhydroxides display negative surface charges under a wide range of pH values and redox conditions (Kosmulski, 2016 and cited references), letting these Mn oxyhydroxides be suitable candidates for new B removal strategies. The preferential reactivity of Mn oxy-hydroxide surfaces towards dissolved metal species (Stumm, 1992) effectively corresponds to the specific framework of low crystalline Mn oxyhydroxide minerals where MnO_6 octahedra share corners or edges (Varentsov and Grasselly, 1980).

For the Platani River, we have estimated that the mineral fraction containing the Mn oxy-hydroxide phase acquires 50% of the available B. Compared to the rubber nanoparticle process, which should not exceed 75% (Babiker et al., 2019), the Mn oxy-hydroxide mineral is promising for removing the B excess from wastewaters, and the identified natural process may potentially open new directions for sustainable remediation processes.

6. Conclusions

B and Li are metal ions with highly stable aqueous species in a wide range of physical-chemical conditions. In Platani river waters, the extent of these conditions was tested by investigating the effects of the ionic strength and water-riverbed sediment interactions on B and Li behaviour in the dissolved phase. The results obtained suggest that B and Li are not significantly fractionated with each other between colloids and the total dissolved fraction under ionic strengths up to 3.9 M, whereas the ionic strength influences the aqueous concentration of these elements. This finding is confirmed by higher values of the B/Li ratio at ionic strengths below 0.5 M and lower B/Li values at ionic strengths above 0.5 M. Accordingly, larger dissolved B–Li fractionations occur in river waters closer to the landfill of Bosco S. Cataldo mine where the effects of the salts weathering is larger. The B–Li fractionation decreases in river waters collected far from the landfill along the river stem where the effect of salt weathering is less evident.

According to the B speciation in the waters studied and comparing B/Li values measured in total dissolved fractions and in fractions extracted from sediments, the formation of borate-ion pairs under high ionic strength conditions increases the reactivity of B-bearing species with surfaces of Mn-rich solids from sediments. This is confirmed by comparing the B/Li ratio and the ionic strength of river waters with those reported in oxic brines equilibrated with Mn-oxyhydroxides.

Data availability

Data will be made available on request.

Declaration of competing interest

The authors declare that they have no known competing financial interests or personal relationships that could have appeared to influence the work reported in this paper.

Acknowledgements

This work was financially supported by the grants CORI 2017 and CON-0037 of the University of Palermo.

Appendix A. Supplementary data

Supplementary data to this article can be found online at https://doi.org/10.1016/j.chemosphere.2022.135509.

References

Babiker, E., Al-Ghouti, M.A., Zouari, N., McKay, G., 2019. Removal of B from water using adsorbents derived from waste tire rubber. Jour. Environ. Chem. Engen. 7, art. no. 102948.

Bhagyaraj, S., Al-Ghouti, M.A., Kasak, P., Krupa, I., 2021. An updated review on B removal from water through adsorption processes. Emergent Mater. 4, 1167–1186.

Bingham, F.T., Page, A.L., 1971. Specific character of B adsorption by an amorphous soil. Soil Sci. Soc. Am. Proc. 35, 892–893.

Brantley, S.L., Conrad, C.F., 2008. Analysis of rates of geochemical reactions. In: Brantley, S.L., Kubicki, J.D., White, A.F. (Eds.), Kinetics of Water-Rock Interaction. Spinger Science Business media, pp. 1–37.

Brodskii, V.A., Gubin, A.F., Kolesnikov, A.V., Makarov, N.A., 2015. Electro-surface properties of metal oxides and hydroxides in water solutions. Glass Ceram. 72, 220–224.

Byrne Jr., R.H., Kester, D.R., 1974. Inorganic speciation of B in seawater. J. Mar. Res. 32, 119–127.

Cozzarelli, I.M., Skalak, K.J., Kent, D.B., Engl, M.A., Benthem, A., Mumford, A.C., et al., 2017. Environmental signatures and effects of an oil and gas wastewater spill in the Williston Basin, North Dakota. Sci. Total Environ. 579, 1781–1793.

Cullen, J.T., Hurwitz, S., Barnes, J.D., Lassiter, J.C., Penniston-Dorland, S., Kasemann, S.A., Thordsen, J.J., 2019. Temperature-dependent variations in mineralogy, major element chemistry and the stable isotopes of B, Li and chlorine resulting from hydration of rhyolite: constraints from hydrothermal experiments at 150 to 350 °C and 25 MPa. Geochem. Cosmochim. Acta 261, 269–287.

Deng, F., Zeng, F., Chen, G., Feng, X., Riaz, A., Wu, X., Gao, W., Wu, F., Holford, P., Chen, Z.-H., 2021. Metalloid hazards: from plant molecular evolution to mitigation strategies. J. Hazard Mater. 409, art. no. 124495.

Dessau, G., Jensen, M.L., Nakai, N., 1962. Geology and isotopic studies of Sicilian sulfur deposits. Econ. Geol. 57, 410–438.

Domínguez Ortega, L., Medina Ortiz, O., Cabrera García-Armenter, S., 2006. Li intoxication [Intoxicación con litio.]. An. Med. Int. 23, 441–445.

Elmaci, G., Icten, O., Nedim, A., Zümreoglu-Karan, B., 2015. B isotopic fractionation in aqueous boric acid solutions over synthetic minerals: effect of layer and surface charge on fractionation factor. Appl. Clay Sci. 107, 117–121.

Gaillardet, J., Viers, J., Dupré, B., 2013. Trace elements in river waters. Treatise Geochem. 7, 195–235, second ed..

Gavrieli, I., Halicz, L., 2002. Limnological changes in depth distributions of uranium and rare earth elements in a hypersaline brine: the Dead Sea. Isr. J. Earth Sci. 51, 243–251, Geosciences 5, 127-140.

Godfrey, L., Álvarez-Amado, F., 2020. Volcanic and saline Li inputs to the Salar de Atacama. Minerals 10 (10), 201. https://doi.org/10.3390/min10020201.

Godfrey, L.V., Herrera, C., Gamboa, C., Mathur, R., 2019. Chemical and isotopic evolution of groundwater through the active Andean arc of Northern Chile. Chem. Geol. 518, 32–44.

Goldberg, S., 1997. Reactions of B with soils. Soils Plants 193, 35–48.

Guo, L., Santschi, P.H., 2007. Ultrafiltration and its applications to sampling and characterisation of aquatic colloids. In: Wilkinson, K.J., Lead, J.R. (Eds.), Environmental Colloids and Particles: Behaviour, Separation and Characterisation. vol. 10, IUPAC Series on Analytical and Physical Chemistry, pp. 160–221.

Hasenmueller, E.A., Criss, R.E., 2013. Multiple sources of B in urban surface waters and groundwaters. Sci. Total Environ. 447, 235–247.

Herut, B., Gavrieli, I., Halicz, L., 1997. Sources and distribution of trace and minor elements in the western dead sea surface sediments. Appl. Geochem. 12, 497–505.

Hoyer, M., Kummer, N.A., Merkel, B., 2015. Sorption of Li on Bentonite, Kaolin and Zeolite.

Ince, S., Filazi, A., Yurdakok-Dikmen, B., 2017. BIn: second ed., Reproductive and Developmental Toxicology, vol. 30, Elsevier, pp. 521–535.

Khosravi, R., Zarei, M., Sracek, O., Bigalke, M., 2019. Geochemical and hydrological controls of arsenic concentrations across the sediment–water interface at Maharlu Lake, Southern Iran. Appl. Geochem. 102, 88–101.

Kochkodan, V., Bin Darwish, N., Hilal, N., 2015. The chemistry of B in water. In: Kabay, N., Bryjak, M., Hilal, N. (Eds.), B Separation Processes. Elsevier, pp. 35–63.

Koschinsky, A., Halbach, P., 1995. Sequential leaching of marine ferromanganese precipitates: genetic implications. Geochem. Cosmochim. Acta 59, 5113–5132.

Kosmulski, M., 2002. The pH-dependent surface charging and the points of zero charge. J. Colloid Interface Sci. 253, 77–87.

Kosmulski, M., 2016. Isoelectric points and points of zero charge of metal (hydr)oxides: 50 years after Parks' review. Adv. Colloid Interface Sci. 238, 1–61.

Larsson, J., Gustafsson, , Ingri, J., 2002. Evaluation and optimization of two complementary cross-flow ultrafiltration systems toward isolation of coastal surface water colloids. Environ. Sci. Technol. 36, 2236–2241.

Lewis, G.N., Randall, M., 1921. The activity coefficient of strong electrolytes. J. Am. Chem. Soc. 43, 1112–1154.

Mandal, B., De, D.K., 1993. Depthwise distribution of extractable B in some acidic inceptisols of India. Soil Sci. 155, 256–262.

McCaffrey, A., Lazar, B., Holland, D., 1987. The evaporation path of seawater and the coprecipitation of Br^- and K^+ with halite. J. Sediment. Petrol. 57, 928–937.

Millot, R., Vigier, N., Gaillardet, J., 2010. Behaviour of Li and its isotopes during weathering in the Mackenzie basin, Canada. Geochem. Cosmochim. Acta 74, 3897–3912.

Navarro-Martínez, F., Sánchez-Martos, F., Salas García, A., Gisbert Gallego, J., 2020. The use of major, trace elements and uranium isotopic ratio ($^{234}U/^{238}U$) for tracing of hydrogeochemical evolution of surface waters in the Andarax River catchment (SE Spain). J. Geochem. Explor. 213, art. no. 106533.

Nir, O., Marvin, E., Lahav, O., 2014. Accurate and self-consistent procedure for determining pH in seawater desalination brines and its manifestation in reverse osmosis modeling. Water Res. 64, 187–195.

Nir, O., Lahav, O., 2015. Single SWRO pass B removal at high pH: prospects and challenges. In: Kabay, N., Bryjak, M., Hilal, N. (Eds.), B Separation Processes. Elsevier, pp. 297–323.

Nishri, A., Nissenbaum, A., 1993. Formation of manganese oxyhydroxides on the Dead Sea coast by alteration of Mn-enriched carbonates. Hydrobiologia 267, 61–73.

Parans Paranthaman, M., Ling, L., Luo, J., Hole, T., Ucar, H., Moyer, B.A., Harrison, S., 2017. Recovery of Li from geothermal brine with Li–Aluminum layered double hydroxide chloride sorbents. Environ. Sci. Technol. 51, 13481–13486.

Parkhurst, D.L., Appelo, C.A.J., 2010. User's Guide to PHREEQC (Version 2.17.5) - A Computer Program for Speciation, Batch- Reaction, One-Dimensional Transport and Inverse Geochemical Calculations, Available at: http://www.brr.cr.usgs.gov/projects/GWC_coupled/phreeqc/index.html.

Qin, Z., Liu, F., Lan, S., Li, W., Yin, H., Zheng, L., et al., 2019. Effect of γ-manganite particle size on Zn^{2+} coordination environment during adsorption and desorption. Appl. Clay Sci. 168, 68–76.

Roden, E.E., 2008. Microbiological controls on geochemical kinetics 1: fundamentals and case study on microbial Fe(III) oxide reduction. In: Brantley, S.L., Kubicki, J.D., White, A.F. (Eds.), Kinetics of Water-Rock Interaction. Spinger Science Business media, pp. 335–416.

Ryan, J.G., Langmuir, C.H., 1993. The systematics of B abundances in young volcanic rocks. Geochem. Cosmochim. Acta 57, 1489–1498.

Sanjuan, B., Gourcerol, B., Millot, R., Rettenmaier, D., Jeandel, E., Rombaut, A., 2022. Lithium-rich geothermal brines in Europe: an up-date about geochemical characteristics and implications for potential Li resources. Geothermics 101, art. no. 102385.

Schlitzer, R., 2015. Ocean Data View. http://odv.awi.de.

Schrauzer, G.N., 2002. Li: occurrence, dietary intakes, nutritional essentiality. J. Am. Coll. Nutr. 21, 14–21.

Stoffyn, M., Mackenzie, F.T., 1982. Fate of dissolved aluminium in the oceans. Mar. Chem. 11, 105–127.

Stumm, W., 1992. Chemistry of the Solid-Water Interface: Processes at the Mineral-Water and Particle-Water Interface in Natural Systems. John Wiley & Sons, Inc.

Sun, Y., Smrzka, D., Peckmann, J., Huang, H., Roberts, H.H., Chen, D., 2021. Uptake of trace elements into authigenic carbonate at a brine seep in the northern Gulf of Mexico. Chem. Geol. 582, art. n° 120442.

Tepavitcharova, S., Todorov, T., Rabadjieva, D., Dassenakis, M., Paraskevopoulou, V., 2011. Chemical speciation in natural and brine sea waters. Environ. Monit. Assess. 180, 217–227.

Tessier, A., Campbell, P.G.C., Bisson, M., 1979. Sequential extraction procedure for the speciation of particulate trace metals. Anal. Chem. 51, 844–851.

Tsadilas, C.D., Dimoyiannis, D., Samaras, V., 1998. B sorption by manganese oxide-coated sand. Commun. Soil Sci. Plant Anal. 29, 2347–2353.

Varentsov, I.M., Grasselly, G. (Eds.), 1980. Geology and Geochemistry of Manganese.

Vengosh, A., Starinsky, A., Kolodny, Y., Chivas, A.R., 1991. B isotope geochemistry as a tracer for the evolution of brines and associated hot springs from the Dead Sea. Israel. Geochim. Cosmochim. Acta 55, 1689–1695.

Vengosh, A., Kolodny, Y., Spivack, A.J., 1998. B Isotope Systematics of Ground-Water Pollution, Applications of Isotopic Techniques to Investigate Ground-Water Pollution. 17–37, Vienna.

Villalobos, M., 2015. The role of surface edge sites in metal(loid) sorption to poorly-crystalline birnessites. ACS (Am. Chem. Soc.) Symp. Ser. 1197, 65–87.

Wang, C., Kong, Z., Duan, L., Deng, F., Chen, Y., Quan, S., Liu, X., Cha, Y., Gong, Y., Wang, C., Shi, Y., Gu, W., Fu, Y., Liang, D., Giesy, J.P., Zhang, H., Tang, S., 2021. Reproductive toxicity and metabolic perturbations in male rats exposed to B. Sci. Total Environ. 785, art. no. 147370.

WHO (World Health Organization), 2017. Guidelines for Drinking-Water Quality: First Addendum to the, fourth ed. fourth ed., +1st add.

Wimpenny, J., James, R.H., Burton, K.W., Gannoun, A., Mokadem, F., Gíslason, S.R., 2010a. Glacial effects on weathering processes: new insights from the elemental and Li isotopic composition of West Greenland rivers. Earth Planet Sci. Lett. 290, 427–437.

Zilberman, T., Gavrieli, I., Yechieli, Y., Gertman, I., Katz, A., 2017. Constraints on evaporation and dilution of terminal, hypersaline lakes under negative water balance: the Dead Sea, Israel. Geochem. Cosmochim. Acta 217, 384–398.